

Isomerically Pure Tetramethylrhodamine Voltage Reporters

Parker E. Deal,[†] Rishikesh U. Kulkarni,[†] Sarah H. Al-Abdullatif,[†] and Evan W. Miller^{*,†,‡,§}

[†]Department of Chemistry, [‡]Department of Molecular & Cell Biology, and [§]Helen Wills Neuroscience Institute, University of California, Berkeley, California 94720, United States

S Supporting Information

ABSTRACT: We present the design, synthesis, and application of a new family of fluorescent voltage indicators based on isomerically pure tetramethylrhodamines. These new Rhodamine Voltage Reporters, or RhoVRs, use photoinduced electron transfer (PeT) as a trigger for voltage sensing, display excitation and emission profiles in the green to orange region of the visible spectrum, demonstrate high sensitivity to membrane potential changes (up to 47% $\Delta F/F$ per 100 mV), and employ a tertiary amide derived from sarcosine, which aids in membrane localization and simultaneously simplifies the synthetic route to the voltage sensors. The most sensitive of the RhoVR dyes, RhoVR 1, features a methoxy-substituted diethylaniline donor and phenylenevinylene molecular wire at the 5'-position of the rhodamine aryl ring, exhibits the highest voltage sensitivity to date for red-shifted PeT-based voltage sensors, and is compatible with simultaneous imaging alongside green fluorescent protein-based indicators. The discoveries that sarcosine-based tertiary amides in the context of molecular-wire voltage indicators prevent dye internalization and 5'-substituted voltage indicators exhibit improved voltage sensitivity should be broadly applicable to other types of PeT-based voltage-sensitive fluorophores.

Cells expend a large amount of energy to maintain an unequal distribution of ions across the plasma membrane, resulting in a transmembrane voltage or potential (V_m).¹ Fast changes in V_m are responsible for the distinct cellular physiology of neurons and cardiomyocytes, and mounting evidence points to the importance of V_m in shaping fundamental cellular processes, such as differentiation, migration, and division, across a number of cell types.² Traditionally, changes in V_m have been monitored using electrodes, which are highly invasive and limited in throughput.³ Broadly applicable and sensitive optical methods to track V_m would expand our capacity to disentangle the contributions V_m makes to human health and disease.⁴

We have recently undertaken a program to design and apply small-molecule fluorescent dyes that use photoinduced electron transfer (PeT) as a molecular switch to optically monitor changes in V_m . The parent family of sensors includes VoltageFluor (VF) dyes (SI Table 1)^{5–7} and makes use of PeT⁸ through a phenylenevinylene molecular wire to modulate the fluorescence intensity of a sulfonofluorescein-based reporter in a V_m -dependent fashion. More recently, we disclosed the development of Berkeley Red Sensor of Transmembrane potential (BeRST 1) (SI Table 1),⁹ which features the shared phenylenevinylene

molecular wire along with a sulfonated silicon-rhodamine fluorophore. Although some members of the VF dye family display high voltage sensitivity ($\Delta F/F$ of 48–49% per 100 mV change),⁶ their excitation and emission profiles in the cyan to green range limit their application alongside many common optical tools like green fluorescent protein (GFP) and Ca²⁺-sensitive GFPs (GCaMPs).¹⁰ BeRST 1 partially solves this problem of spectral overlap by the use of the far-red/near-infrared Si-rhodamine, but its voltage sensitivity is lower compared with the VF dyes (24% $\Delta F/F$ per 100 mV) and the synthetic route to BeRST 1 is low-yielding because of the inclusion of a sulfonic acid functional group on the *meso*-aryl ring of BeRST 1. We hoped to develop a voltage-sensing scaffold that would retain the high sensitivity of the VF dye series, expand the spectrum of colors available for high-fidelity voltage sensing, and circumvent the inclusion of the sulfonate group that makes synthetic efforts challenging. Toward this end, we disclose the design and synthesis of the Rhodamine Voltage Reporter (RhoVR, “rover”) family of tetramethylrhodamine (TMR)-based PeT voltage indicators. We have synthesized four new RhoVR dyes, which display excitation and emission profiles spectrally distinct from those of both VF and BeRST-type dyes, feature voltage sensitivities $\Delta F/F$ of 3–47% per 100 mV, and make use of an *ortho*-tertiary amide instead of a sulfonate to achieve membrane localization.

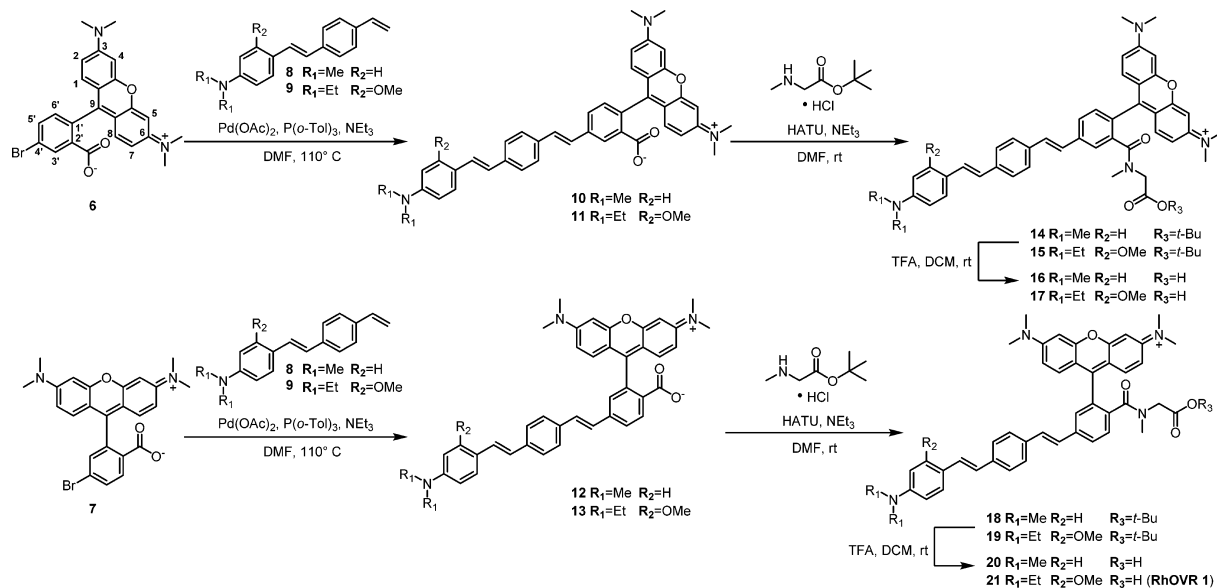
TMR-based voltage indicators were synthesized in isomerically pure form from the 4'- and 5'-bromo TMR derivatives (Scheme 1). We generated isomerically pure rhodamines by condensation of dimethylaminophenol with the corresponding 2-carboxybenzaldehydes 3 and 5 (SI Scheme 1), which were prepared in 79% and 88% yield over a two-step radical bromination followed by hydrolysis of either commercially available 5-bromophthalide 4 or 6-bromophthalide 2 (prepared from commercially available phthalide 1 in 62% yield; SI Scheme 1).^{11,12} Separation of isomers at the 6-bromophthalide stage obviates the need to separate isomers at the rhodamine stage: addition of dimethylaminophenol occurs exclusively at the electrophilic aldehyde carbonyl.¹³ Condensation of dimethylaminophenol with carboxybenzaldehyde in propionic acid in the presence of catalytic PTSA¹³ gave the 4'- and 5'-bromoTMR derivatives in 35% (6) and 57% (7) yield, respectively, after purification by silica gel chromatography (SI Scheme 2). Subsequent Pd-catalyzed Heck coupling with substituted styrenes 8 and 9 (SI Scheme 3) gave the TMR-based voltage sensors in 41–55% yield following silica gel purification. Formation of an *N*-methylglycine-derived tertiary amide

Received: June 2, 2016

Published: July 18, 2016



Scheme 1. Synthesis of Isomerically Pure Rhodamine Voltage Sensors



mediated by HATU gave the *tert*-butyl ester-protected voltage sensors in >70% yield, which exist as mixtures of rotamers around the sarcosinyl–amide bond, as determined by variable-temperature (VT) NMR analysis (SI Figure 1). TFA-catalyzed deprotection of the *tert*-butyl ester gave the final voltage sensors in 7–18% yield over two steps after reversed-phase HPLC purification.

Each RhoVR displayed absorption profiles centered at 564–565 nm ($\epsilon = 70\,000$ to $87\,000\text{ M}^{-1}\text{ cm}^{-1}$ (SI Figure 2). A strong secondary absorption band near 400 nm indicated the presence of the phenylenevinylene molecular wire (SI Figure 2). Emission from all of the RhoVRs was centered at 586–588 nm ($\Phi = 0.89$ – 9.2% ; Table 1). The low Φ values may indicate variable levels of PeT within the compounds.

Table 1. Properties of RhoVRs

compd	$\epsilon/\text{M}^{-1}\text{ cm}^{-1}$ ($\lambda_{\text{max}}/\text{nm}$) ^a	Φ ($\lambda_{\text{max}}/\text{nm}$) ^a	$\Delta F/F$ (100 mV) ^b	SNR (100 mV) ^b
16	75000 (565)	0.036 (586)	$3 \pm 0.2\%$	19:1
17	70000 (565)	0.092 (588)	$26 \pm 3\%$	37:1
20	77000 (564)	0.0089 (586)	$7 \pm 1\%$	96:1
21	87000 (564)	0.045 (588)	$47 \pm 3\%$	160:1

^aPBS, pH 7.2, 0.1% SDS. ^bVoltage-clamped HEK cells.

All of the sarcosine-substituted RhoVRs (500 nM, imaged in dye-free HBSS) localized well to the plasma membrane of HEK cells, as determined by fluorescence microscopy (Figure 1a,b and SI Figures 3–5). Control experiments conducted with TMR derivatives lacking the sarcosine amide (i.e., free carboxylates 10–13) showed strong internal membrane staining (Figure 1a). The dramatic change in cellular localization is consistent with our hypothesis that inclusion of a charged tertiary amide at the *ortho* position of the pendant aryl ring prevents the formation a neutral spirocycle and subsequent cellular dye uptake. The use of carboxylate derivatives drastically simplifies the synthetic route to make long-wavelength voltage indicators.

The voltage sensitivity of each RhoVR was assessed in HEK cells using patch-clamp electrophysiology in whole-cell voltage-clamp mode. Hyper- and depolarizing voltage steps spanning a

range from -100 to $+100$ mV in 20 mV increments from a holding potential of -60 mV provided voltage sensitivities of 3–47%, depending on the dye (Table 1, Figure 1c,d, and SI Figure 6). Compound 21, which we dubbed RhoVR 1, emerged as the most voltage-sensitive dye (Table 1). Dyes bearing methoxy substitution on the aniline (17 and 21) showed improved voltage sensitivity relative to unsubstituted anilines (26% (17) vs 3% (16) and 47% (21, RhoVR 1) vs 7% (20)), as observed for fluorescein-based voltage indicators.⁶ We also observed that voltage indicators derived from 5'-substituted rhodamines were both more voltage-sensitive (47% (21, RhoVR 1) vs 26% (17) and 7% (20) vs 3% (16)) and brighter in cells (SI Figure 3). Studies are underway to probe the nature of this difference. Given the high sensitivity and brightness of RhoVR 1 in cells, we chose this dye to evaluate in subsequent experiments. RhoVR 1 shows photostability comparable to that of VF2.1.Cl (SI Figure 3e).

When bath-applied to cultured rat hippocampal neurons, RhoVR1 gave distinct membrane-associated staining. The clear membrane staining, coupled with the high voltage-sensitivity of RhoVR 1 enabled the detection of spontaneously firing action potentials with an average $\Delta F/F$ of 15% ($N = 27$ spikes) and signal-to-noise ratios (SNRs) ranging from 10:1 to 20:1 that were largely dependent on the illumination intensity used (1.7 to 3.1 W/cm²) (Figure 2, cells 2–5). To confirm that the spiking events we observed arose from action potentials, we treated actively firing cultures with tetrodotoxin (TTX), a sodium channel toxin that inhibits action potential firing, and observed no spiking activity after TTX treatment (SI Figure 7).

RhoVR 1 represents the most sensitive red-shifted PeT-based voltage indicator to date: VF2.1(OMe).Cl has a voltage sensitivity of 49%⁶ but emission at 536 nm, while BeRST 1 has bathochromic emission at 680 nm but a voltage sensitivity of only 24%.⁹ Given the success of far-red voltage dyes like BeRST 1 in integrating multiple functional signals simultaneously, we wondered whether we might be able to perform two-color imaging simultaneously with RhoVR 1 despite the tighter optical overlap between rhodamines and GFP-based chromophores. Expression of cytosolic enhanced GFP (eGFP) in HEK cells stained with RhoVR 1 did not result in significant bleed-through

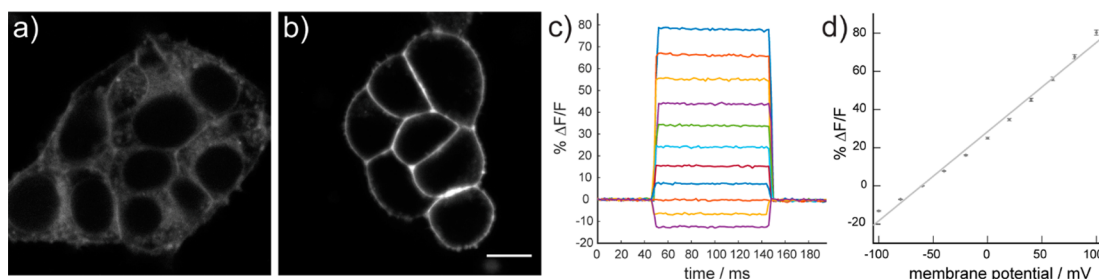


Figure 1. Cellular characterization of rhodamine-based voltage indicators. (a, b) Confocal fluorescence images of HEK cells stained with (a) compound 13 (no sarcosine amide) or (b) RhoVR 1 (compound 21, with sarcosine amide). Incorporation of the tertiary amide based on sarcosine results in a clear enhancement of membrane-localized fluorescence (panel a vs b). The fluorescence of membrane-localized RhoVR 1 is voltage-sensitive. The scale bar is 10 μm . (c) Plot of the fractional change in fluorescence vs time for 100 ms hyper- and depolarizing steps (± 100 mV in 20 mV increments) from a holding potential of -60 mV for single HEK cells under whole-cell voltage-clamp mode. (d) Plot of $\% \Delta F/F$ vs final membrane potential summarizing data from nine separate cells, revealing a voltage sensitivity of approximately 47% per 100 mV. Error bars are \pm SEM.

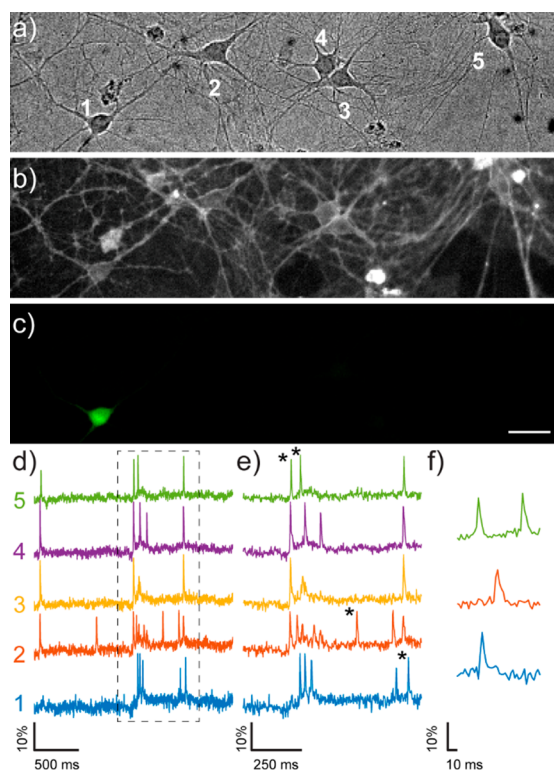


Figure 2. (a–c) Imaging of spontaneous neuronal activity with RhoVR 1 and eGFP. Rat hippocampal neurons (DIC, a) were stained with 500 nM RhoVR (fluorescence, b). A small number of neurons transiently expressed eGFP (fluorescence, c). The scale bar is 20 μm . (d–f) The spontaneous activity of the neurons in panels (a) and (b) were recorded optically at 500 Hz using RhoVR 1. The activity of each neuron (1–5, panel a) is displayed as a trace of fluorescence intensity vs time (d). The boxed regions in (d) are shown on an expanded scale in (e). Asterisks indicate traces expanded in (f).

of eGFP fluorescence into the rhodamine channel and did not substantially diminish the voltage sensitivity of RhoVR-1 in voltage-clamped HEK cells ($47 \pm 3\%$ without vs $45 \pm 1\%$ with eGFP; SI Figure 8). Furthermore, cytosolic eGFP in cultured neurons did not attenuate our ability to track action potentials in spontaneously firing neurons in culture (Figure 2). Indeed, when imaging spontaneous activity in cultured rat hippocampal neurons, we were able to clearly distinguish distinct spiking events arising from neighboring cells (Figure 2b,d, neurons 3 and

4) and clearly resolve spikes in neurons expressing eGFP in single trials (Figure 2b–d, neuron 1).

Encouraged by these results, we next sought to image voltage and Ca^{2+} dynamics simultaneously¹⁴ by exciting the specimen with green and blue light and splitting the resulting emission to capture rhodamine and GFP fluorescence in parallel (SI Scheme 4). Brief rises in intracellular $[\text{Ca}^{2+}]$ (Ca^{2+} transients), on the order of hundreds of milliseconds, are used as a surrogate for neuronal membrane depolarizations and are often monitored with green-fluorescent Ca^{2+} -sensitive fluorophores like the genetically engineered GCaMP6s.¹⁰ We expressed GCaMP6s, on account of its excellent sensitivity to Ca^{2+} released in response to single action potentials,¹⁰ in cultured hippocampal neurons and incubated these neurons with RhoVR 1 (500 nM). Using an image splitter (SI Scheme 4) to separate emitted photons according to wavelength, we recorded Ca^{2+} transients via GCaMP6s fluorescence and voltage spikes via RhoVR 1 fluorescence. Under these conditions, hippocampal neurons again displayed significant amounts of spontaneous spiking activity in multiple distinct neurons, as detected by GCaMP6s (Figure 3a, green) and RhoVR 1 (Figure 3a, magenta).

The sensitivity of RhoVR 1 to these action potentials was similar to values obtained in experiments recorded at a single wavelength alone ($\Delta F/F$ per spike = 9.5%, SNR = 12:1, $N = 70$ spikes; Figure 3a,e–g). Typically, one neuron expressed high levels of GCaMP6s fluorescence in a field of view (Figure 3d), which enabled us to directly compare transient rises in Ca^{2+} with fast voltage spikes in the same neuron (Figure 3a). In all cases, the fast voltage spike clearly precedes the subsequent Ca^{2+} transient. RhoVR 1 displays comparable or better $\Delta F/F$ values for single spikes relative to the corresponding Ca^{2+} transients in the same cell (Figure 3a and SI Movie 1). Because of the inherently fast kinetics of V_m relative to Ca^{2+} , monitoring V_m directly via RhoVR 1 enables resolution and precise timing of spikes occurring in quick succession from multiple cells (Figure 3f–h), which would be impossible using more traditional approaches such as Ca^{2+} imaging or single-cell electrophysiology.

In summary, we have presented the design, synthesis, and application of four members of a new class of voltage-sensitive dyes based on tetramethylrhodamine. All of the new sensors display excitation and emission profiles greater than 550 nm, good photostability, and varying degrees of voltage sensitivity in patch-clamped HEK cells. The best of the new voltage indicators, RhoVR 1, displays a voltage sensitivity $\Delta F/F$ of 47% per 100 mV, rivaling the sensitivity of the fluorescein-based VF2.1(OMe).H ($\Delta F/F = 49\%$ per 100 mV)⁶ and surpassing that of our most red-

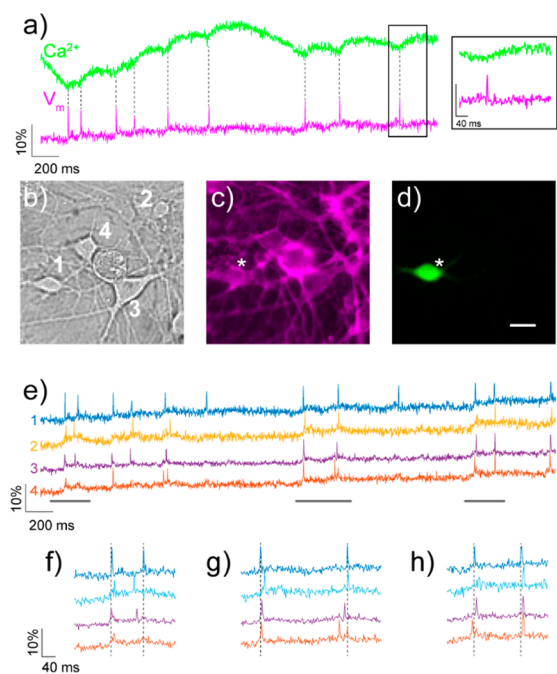


Figure 3. Simultaneous two-color imaging of voltage and Ca^{2+} in hippocampal neurons using RhoVR 1 and GCaMP6s. (a) The green trace shows the relative change in fluorescence from Ca^{2+} -sensitive GCaMP6s, while the magenta trace depicts relative fluorescence changes in RhoVR 1 fluorescence from neuron 1 in (b). The inset shows an expand time scale of the boxed region. (b) DIC image of neurons expressing GCaMP6s and stained with RhoVR 1. (c) Fluorescence image showing membrane localization of RhoVR 1 fluorescence from neurons in (b). (d) Fluorescence image of neurons in (b) showing GCaMP6s fluorescence. Scale bar is $20 \mu\text{m}$. (e) Traces showing the activity of each neuron in (b–d), displayed as the fractional change in voltage-sensitive RhoVR 1 fluorescence vs time. (f–h) Regions of the traces in (e) are shown on an expanded time scale to compare the spike timing of imaged neurons.

shifted probe, BeRST 1 ($\Delta F/F = 24\%$ per 100 mV).⁹ Although the excitation and emission spectra of RhoVR 1 are blue-shifted relative to those of BeRST 1, the TMR optical profile still provides ample spectral separation to perform two-color imaging alongside other optical probes, such as GFP and the GCaMP family of sensors. Using a combination of GCaMP6s and RhoVR 1, we simultaneously imaged Ca^{2+} transients and membrane potential depolarizations in cultured hippocampal neurons, establishing that RhoVR 1 and related compounds will be useful for parsing the roles of Ca^{2+} and V_m in living cells.

Taken together, these data demonstrate the utility of sarcosine-substituted rhodamines dyes for voltage sensing in living cells. The incorporation of the 2'-carboxylate simplifies the synthetic route to long-wavelength voltage sensors by avoiding highly polar sulfonates, which complicate purification, and subsequent modification with sarcosine prevents the internalization that plagues unfunctionalized xanthene-based voltage indicators. Inclusion of the free carboxylate on sarcosine provides a convenient handle for subsequent functionalization and localization to genetically encoded protein partners or delivery agents. Furthermore, expansion of PeT-based voltage indicators to include rhodamines offers a new optical channel for use in voltage sensing and demonstrates the versatility and generality of a PeT-based approach to voltage sensing. We were pleasantly surprised to find that the 5'-substituted rhodamines showed greater voltage sensitivity than the 4'-substituted dye, which has

been the typical substitution pattern for our previous molecular-wire voltage sensors and many PeT-based analyte sensors.^{15–17} Experiments are underway to probe the nature of this voltage sensitivity enhancement as well as to apply this substitution pattern to future generations of voltage-sensitive dyes and other sensing platforms.

■ ASSOCIATED CONTENT

Supporting Information

The Supporting Information is available free of charge on the ACS Publications website at DOI: 10.1021/jacs.6b05672.

Synthetic details and additional data (PDF)

Movie of RhoVR 1 and GCaMP6s fluorescence (AVI)

■ AUTHOR INFORMATION

Corresponding Author

*evanwmiller@berkeley.edu

Notes

The authors declare no competing financial interest.

■ ACKNOWLEDGMENTS

The authors acknowledge generous support from the University of California, Berkeley, the Hellman Foundation, the March of Dimes (5-FY16-65), the Alzheimer's Association (2016-NIRG-394290), and the NIH (R00 NS07581). R.U.K. was supported in part by an NIH Chemical Biology Training Grant (T32 GM066698). Confocal imaging was performed at the CRL Molecular Imaging Center, UC Berkeley, supported by the Helen Wills Neuroscience Institute. We thank Dr. Alison Walker and Pei Liu for expert technical assistance with neuronal cultures and Dr. Hasan Celik for help with VT-NMR studies.

■ REFERENCES

- (1) Engl, E.; Attwell, D. *J. Physiol.* **2015**, *593*, 3417.
- (2) Levin, M. *Mol. Biol. Cell* **2014**, *25*, 3835.
- (3) Peterka, D. S.; Takahashi, H.; Yuste, R. *Neuron* **2011**, *69*, 9.
- (4) (a) Braubach, O.; Cohen, L. B.; Choi, Y. *Adv. Exp. Med. Biol.* **2015**, *859*, 3. (b) Loew, L. M. *Adv. Exp. Med. Biol.* **2015**, *859*, 27. (c) Miller, E. W. *Curr. Opin. Chem. Biol.* **2016**, *33*, 74.
- (5) Miller, E. W.; Lin, J. Y.; Frady, E. P.; Steinbach, P. A.; Kristan, W. B., Jr.; Tsien, R. Y. *Proc. Natl. Acad. Sci. U. S. A.* **2012**, *109*, 2114.
- (6) Woodford, C. R.; Frady, E. P.; Smith, R. S.; Morey, B.; Canzi, G.; Palida, S. F.; Araneda, R. C.; Kristan, W. B., Jr.; Kubiak, C. P.; Miller, E. W.; Tsien, R. Y. *J. Am. Chem. Soc.* **2015**, *137*, 1817.
- (7) Grenier, V.; Walker, A. S.; Miller, E. W. *J. Am. Chem. Soc.* **2015**, *137*, 10894.
- (8) Li, L. S. *Nano Lett.* **2007**, *7*, 2981.
- (9) Huang, Y.-L.; Walker, A. S.; Miller, E. W. *J. Am. Chem. Soc.* **2015**, *137*, 10767.
- (10) Chen, T. W.; Wardill, T. J.; Sun, Y.; Pulver, S. R.; Renninger, S. L.; Baohan, A.; Schreiter, E. R.; Kerr, R. A.; Orger, M. B.; Jayaraman, V.; Looger, L. L.; Svoboda, K.; Kim, D. S. *Nature* **2013**, *499*, 295.
- (11) Mirabdolbaghi, R.; Dudding, T. *Org. Lett.* **2012**, *14*, 3748.
- (12) Clark, R. B.; Hunt, D. K.; Plamondon, L.; Sun, C.; Xiao, X.-Y.; Roenn, M. (Tetraphase Pharmaceuticals). WO2010132670A2, 2010.
- (13) Mudd, G.; Pi, I. P.; Fethers, N.; Dodd, P. G.; Barbeau, O. R.; Auer, M. *Methods Appl. Fluoresc.* **2015**, *3*, 045002.
- (14) Jaafari, N.; Vogt, K. E.; Saggau, P.; Leslie, L. M.; Zecevic, D.; Canepari, M. *Adv. Exp. Med. Biol.* **2015**, *859*, 103.
- (15) Minta, A.; Kao, J. P. Y.; Tsien, R. Y. *J. Biol. Chem.* **1989**, *264*, 8171.
- (16) Dodani, S. C.; He, Q. W.; Chang, C. J. *J. Am. Chem. Soc.* **2009**, *131*, 18020.
- (17) Egawa, T.; Hirabayashi, K.; Koide, Y.; Kobayashi, C.; Takahashi, N.; Mineno, T.; Terai, T.; Ueno, T.; Komatsu, T.; Ikegaya, Y.; Matsuki, N.; Nagano, T.; Hanaoka, K. *Angew. Chem., Int. Ed.* **2013**, *52*, 3874.